Available online at www.sciencedirect.com
SCIENCE DIRECT®
Acta Biomaterialia 2 (2006) 343–348
Acta BIOMATERIALIA
www.actamat-journals.com

Combining particle size distribution and isothermal calorimetry data to determine the reaction kinetics of α-tricalcium phosphate–water mixtures

Marc Bohner *, Anna K. Malsy, Christopher L. Camiré, Uwe Gbureck

Dr. H.C. Robert Mathys Foundation, Bischmattstrasse 12, Bettlach 2544, Switzerland

Received 7 September 2005; received in revised form 11 January 2006; accepted 12 January 2006

Abstract

Many calcium phosphate bone substitutes are based on the use of α-tricalcium phosphate (α-TCP) powder. This compound has been intensively studied, but some aspects of α-TCP reactivity are still controversial. The goal of this study was to determine the setting kinetics of α-TCP based on a new approach that compared particle size distribution data to isothermal calorimetry data. Results indicated that α-TCP conversion is mostly controlled by surface reactions, with at later stages a diffusion-controlled mechanism. The presence of an X-ray amorphous α-TCP fraction in the crystalline α-TCP powder increased the dissolution rate threefold, without modifying the reaction mechanism.
© 2006 Acta Materialia Inc. Published by Elsevier Ltd. All rights reserved.

Keywords: Calcium phosphate; Cement; Kinetics; Particle size distribution; Bone substitute

1. Introduction

Many formulations of hydraulic calcium phosphate cements contain α-tricalcium phosphate (α-TCP) powder as the main component. As a result, the hydraulic properties of α-TCP have been analyzed by several authors. In 1996 and 1997, respectively, Fernandez and Ginebra et al. [1,2] observed that the compressive strength and extent of reaction increased linearly with time, subsequently reaching a saturation level. In 1999, the latter authors refined their analysis based on the particle size distribution of α-TCP powder [3]. It was concluded that the reaction was initially controlled by α-TCP surface area, and then by the diffusion of reactants through the hydrated layer around α-TCP particles. Similar results were obtained by Sarda et al. [4]. Durucan and Brown [5] proposed a slightly different interpretation of the hydrolysis reaction of α-TCP: α-TCP hydrolysis reaction was believed to be initially controlled by a surface-controlled mechanism, and later on by the rate of apatite formation according to a nucleation and growth mechanism.

Despite in-depth studies there is still little known about the effect of the synthesis conditions of α-TCP powders on their reactivity. Ginebra et al. [6] and Ducuran and Brown [7] showed that the setting reaction was accelerated when α-TCP powder was exposed to longer milling times. Recently, Gbureck et al. [8] demonstrated that prolonged milling of α-TCP led to the formation of an X-ray amorphous α-TCP which had a solubility three times that of standard α-TCP. Camiré et al. [9] related milling time and reactivity as measured by isothermal calorimetry. It was found that the total heat released during the conversion of α-TCP into calcium-deficient hydroxyapatite (CDHA) was increased two- to threefold when α-TCP was milled for a prolonged time. However, no kinetics data were presented. Therefore, the aim of the present study was to analyze the reaction kinetics of the α-TCP transformation into CDHA with respect to the milling conditions of the α-TCP powder.

* Corresponding author. Tel.: +41 326441413.
E-mail address: marc.bohner@rms-foundation.ch (M. Bohner).

1742-7061/$ - see front matter © 2006 Acta Materialia Inc. Published by Elsevier Ltd. All rights reserved.
doi:10.1016/j.actbio.2006.01.003

2. Materials and methods

The α-TCP powders used in the present study were the same as those used in a previous study [9]. An in depth description of materials and methods can be found in the latter document, and only a brief description is given here. Two α-TCP batches were produced from 2:1 molar mixtures of calcium carbonate (Merck, Germany, Art 102076) and dicalcium phosphate (first batch: Merck Art No 112076; second batch: Aldrich, Switzerland, Art 23475). The first powder (batch 1) was produced by Synthes Biomaterials (Bettlach, Switzerland), whereas the second powder was produced at the Robert Mathys Foundation. Both powders underwent a heating cycle characterized by a calcination at 900 °C (1 h), followed by a de-agglomeration step (with a pestle and a mortar until all particles passed a 0.5 mm sieve), and a final calcination at 1350 °C for 4 h. As α-TCP is a high-temperature phase metastable at room temperature, the powder was removed from the furnace at 1200 °C and quenched in air. Both batches were then milled according to two different routes. The powder of batch 1 was crushed by hand until all particles passed through a 2 mm sieve, and then milled by ball milling at 60 revolutions per minute (rpm) in ethanol (300 g ethanol, 370 g α-TCP powder, and 2.3 kg ZrO_2 beads; 2 L polyethylene containers—diameter 11 cm). The ethanol had a relatively low purity (96.2% ethanol, 3.6% methanol) for cost reasons. The powder–alcohol mixture was then sieved through a 0.5 mm sieve to remove the beads, and dried in a well-ventilated oven at 60 °C. Even though the latter powder is normally used as such, the powder was milled in a planetary mill (Pulverisette 5, Fritsch, Germany) using ZrO_2 spheres (weight: 3 g each) for 3, 7, 15, 30 and 45 min (100 g powder, 100 ZrO_2 beads, rotation speed: 400 rpm). The powder of batch 2 was milled with a jaw crusher (Pulverisette 1, Fritsch, Germany), and then by hand with a pestle and a mortar until all particles passed through a 2 mm sieve. The latter powder could not be used as such, and had to be milled additionally with the planetary mill for 15, 30, 75, 150 and 225 min with the same parameters as for batch 1.

In this paper, the milling time is arbitrarily defined as the duration of milling in the planetary mill. Therefore, the powder of batch 1 milled for 15 min had sustained a longer total milling time than the powder of batch 2 milled for 15 min. Nevertheless, the first study [9] demonstrated that the powders of batch 1 and batch 2 milled for the same duration in the planetary mill behaved very similarly.

Materials were characterized in a number of ways. The specific surface area (SSA) of the powders was determined using nitrogen adsorption and applying the Brunauer–Emmett–Teller theory (Gemini 2360, Micromeritics, USA). Particle size distribution (PSD) was determined using a laser particle size analysis (L300, Horiba, Kyoto, Japan). Three measurements were performed per powder. The average of these three measurements was subsequently used for the determination of the setting kinetics. No β-TCP could be detected in any of the powders and only negligible amounts of HA were detected in the first α-TCP batch. The crystal size of the α-TCP powders was estimated from the X-ray diffraction (XRD) spectra using the peak breadth at half maximum (FWHM) of two neighboring peaks ((i) at $d = 2.619$ (43% peak according to JCPDS file 23–359) and (ii) at $d = 2.600$ (29% peak)) and the Scherrer equation. The crystal size decreased from about 60 nm at 3 min milling down to 25 nm at 225 min milling. Thermal behavior of milled α-TCP powders up to 500 °C was determined via differential scanning calorimetry (Mettler TA 4000 with measuring cell DSC-20; Switzerland). Differential scanning calorimetry up to 1500 °C was performed at a heating rate of 10 °C/min (Model STA 409, Netsch, Germany). Isothermal calorimetry tests were performed at physiological temperature by hydrating 1 g samples with a liquid to powder ratio of 1:3 with a 2.5% Na_2HPO_4 solution. The crystalline composition of the milled powders and the degree of conversion of set cements was measured for three powders (batch 1: 3 min milling, and batch 2: 15 min and 150 min milling times, respectively; there was too little powder left for most samples to allow such an analysis for all powders) using X-ray diffraction analysis (Siemens D5005, Karlsruhe, Germany) using CuKα radiation. 1.5 g of powder was mixed with 530 μl of a 2.5% Na_2HPO_4 solution on a glass slab and the paste was afterwards hardened at 37 °C and 100% relative humidity for defined time periods of 30 min, 1, 2, 4, 8, 16 and 24 h. The hardened cement was then ground in acetone to stop the setting reaction and dried in air following XRD analysis. The phase composition of the set cements was calculated using Rietveld refinement analysis (TOPAS2, Bruker AXS, Karlsruhe, Germany). As references the system internal database structures of α-TCP (PDF No. 09-0348) and CDHA (PDF No. 09-0432) were used together with a Chebychev forth order background model and a CuK_α emission profile.

In the previous publication [9], the PSD and calorimetric data were not fully explored. In that case, only mean particle size and exotherm were considered. Here, the goal was to relate the PSD to the calorimetric data in order to determine the reaction kinetics. For that purpose, two main assumptions were made: (i) the dissolution rate of each particle was independent of its size and (ii) the degree of reaction, α, was proportional to the amount of heat released during the hydraulic reaction. To relate the reacted layer thickness to the reaction time, the same method as that presented by Ginebra et al. [3] was used. To simplify, two functions were used

$$\alpha = f_1(t), \tag{1}$$

where α is the degree of reaction at a time t during the calorimetry experiment, and $f_1(t)$ is a function of t. The second function, f_2, relates the dissolution depth, δ, of α-TCP particles to the degree of reaction

$$\delta = f_2(\alpha). \tag{2}$$

This function can be calculated from the PSD of each α-TCP powder assuming that particles are spherical and that the linear dissolution rate is independent of the particle size. Eqs. (1) and (2) can be combined to obtain

$$\delta = f_2(f_1(t)). \quad (3)$$

Eq. (3) relates the depth of reaction to the reaction time. With this relationship, it is possible to determine the reaction kinetics. For example, if the reaction is controlled by the surface area of α-TCP powder, a linear relationship should be found between δ and t ($\delta = k_1(t)$ where k_1 is a constant). If the reaction is controlled by diffusion, Eq. (3) should be parabolic ($\delta = k_2(t)^{1/2}$ where k_2 is a constant).

3. Results

The PSD of α-TCP powders was bimodal with peaks close to 1 and 10 μm (Figs. 1 and 2). An increase of milling time tended to decrease the size of the second peak (Figs. 1 and 2) even though the powders milled for 75 and 150 min had a larger second peak than the powder milled for only 15 and 30 min (Fig. 2). This was expressed by a minimum of particle size at an intermediate (30–45 min) milling time (Table 1).

All calorimetry curves typically presented two peaks: one large and narrow peak after about 10 min and one broad and flat peak after 1–2 h (Figs. 3 and 4). The height of the two peaks depended on milling time: the first peak tended to increase in size with an increase in milling time, whereas the second peak tended to decrease in size. Interestingly, the total released heat increased with an increase in milling time, as previously reported [9].

The dissolution depth calculated from the data varied almost linearly as a function of reaction time (Fig. 5). At long reaction times and short milling times, the slope of the curve tended to decrease in a somewhat parabolic fashion. When the slope of the linear domain was computed, it appeared that the slope was close to 0.8 μm/h for milling times shorter than or equal to 45 min, and close to 2.5 μm/h at 75 min milling time and beyond (Fig. 6). It is

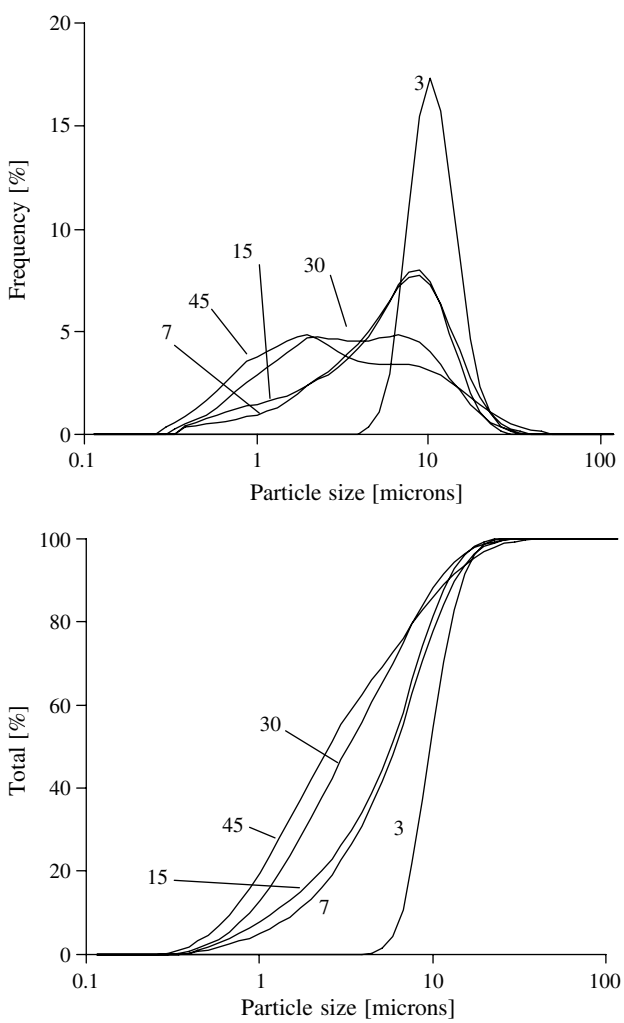

Fig. 1. Particle diameter distribution (in volume) as a function of milling time for the first batch (see Table 1). Top: frequency plot. Bottom: cumulative plot. Milling times: 3, 7, 15, 30 and 45 min.

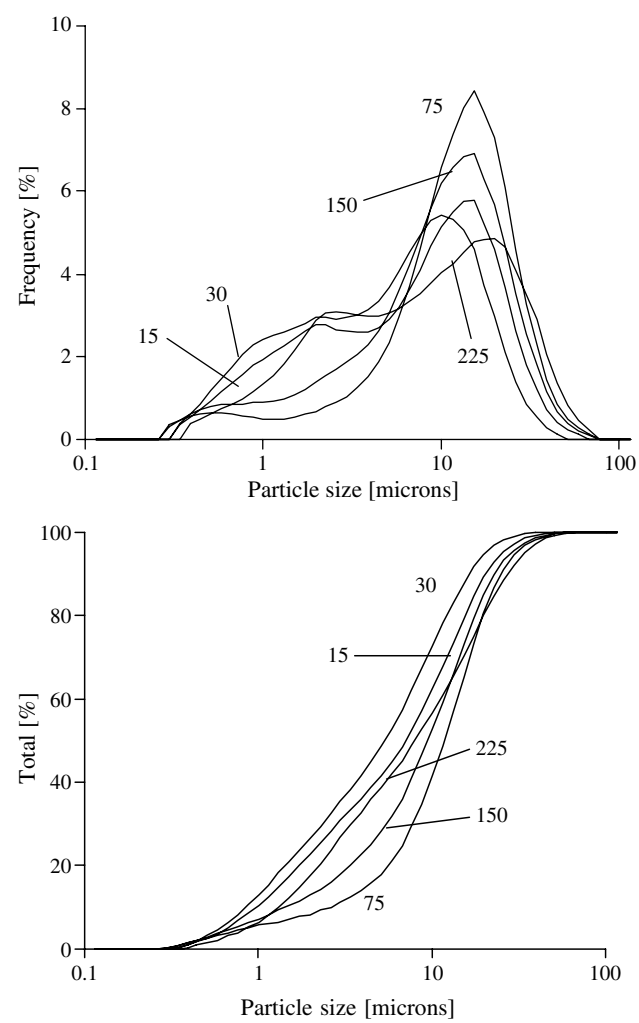

Fig. 2. Particle diameter distribution (in volume) as a function of milling time for the second batch (see Table 1). Top: frequency plot. Bottom: cumulative plot. Milling times: 15, 30, 75, 150 and 225 min.

Table 1
Main features of the α-TCP powders used in the present study

Batch no. and denomination	Milling time (min)	Particle size (μm)	SSA (calc) (m^2/g)	SSA (meas) (m^2/g)	Reacted fraction (%)
1 1024	3	9.6 ± 0.5	0.21	1.31 ± 0.03	28
1 1025	7	6.1 ± 0.2	0.57	1.97 ± 0.03	49
1 1020	15	5.8 ± 0.4	0.66	2.50 ± 0.04	52
1 1022	30	3.5 ± 0.3	0.95	2.38 ± 0.11	65
1 1023	45	2.6 ± 0.5	1.18	2.34 ± 0.05	69
2 19	15	7.1 ± 0.8	0.72	1.93 ± 0.06	49
2 1032	30	5.1 ± 1.0	0.84	2.45 ± 0.05	55
2 1033	75	11.9 ± 0.6	0.44	2.28 ± 0.06	33
2 1034	150	9.2 ± 0.7	0.56	2.16 ± 0.04	39
2 1035	225	8.5 ± 0.2	0.58	2.28 ± 0.07	45

(i) Milling time; (ii) particle size; (iii) specific surface area (SSA) calculated from the particle size distribution (PSD; assuming spherical particles); (iv) measured SSA; (v) reacted fraction with a dissolution depth of 1 μm (calculated from the PSD assuming that the particles are spherical). Most of the results presented in this table were previously presented in Ref. [9].

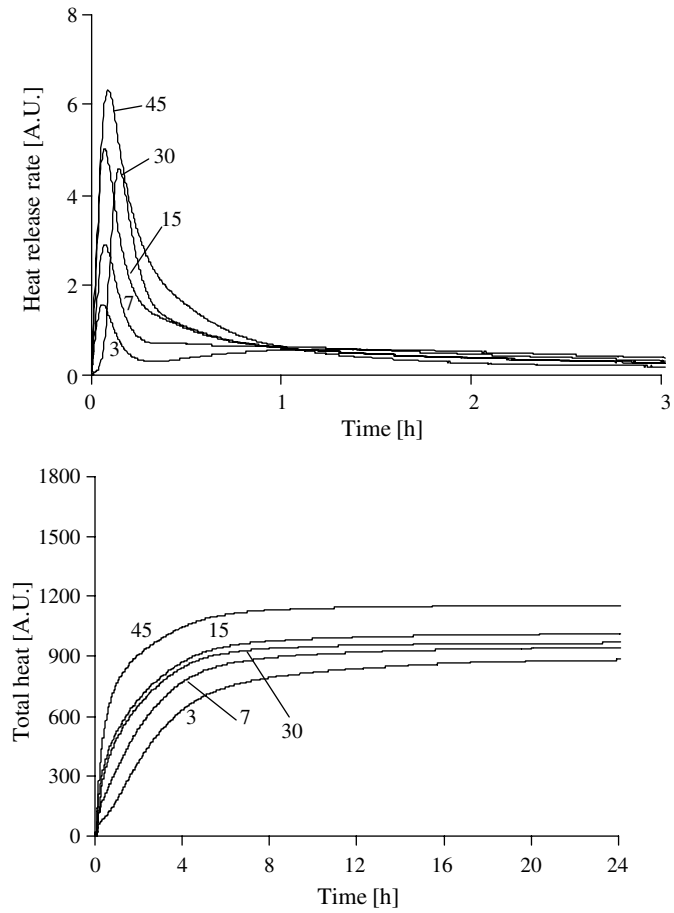

Fig. 3. Isothermal calorimetry curves of the first batch (see Table 1). Milling times: 3, 7, 30, 15 and 45 min. Top: frequency plot. Bottom: cumulative plot. The heat release rate and total heat are given in arbitrary units (raw signal in mV and mV s, respectively).

noteworthy that dissolution depths up to 8 μm were indicated for all powders even though the average particle size for some powders was lower than 8 μm. This is due to the fact that all powders contained small (submicron range) and large (>8 μm) particles.

In the present study, only one calorimetry measurement was performed per composition, which does not allow assessment of data reproducibility and significance of the results of Fig. 6. It was concluded that the results were accurate and significant after results obtained by the initial investigator were confirmed on a different instrument by another investigator (M. Bohner). Tests were carried out with the same powders in 0.2 M Na_2HPO_4 (at least three measurements per powder). Very similar results were obtained with 0.2 M Na_2HPO_4 compared to 2.5% Na_2HPO_4, i.e. the kinetics and dissolution rate were identical, hence supporting the conclusions of the present study.

4. Discussion

Three types of information were obtained in this study: (i) PSD data, (ii) calorimetric data, and (iii) the combination of PSD and calorimetric data to reveal setting kinetics and calculate both depth of reaction and percentage reacted volume. The results presented suggest that α-TCP hydrolysis is mostly surface-controlled, as evidenced by the linear evolution of the dissolution depth as a function of dissolution time (Fig. 5). Moreover, the linear domain became more extensive at longer milling times. Both results are in agreement with those of Ginebra et al. [3,6], but disagree with those of Durucan and Brown [5] who concluded that α-TCP hydrolysis reaction was initially controlled by a surface-controlled mechanism, and later on by the rate of apatite formation according to a nucleation and growth mechanism. However, the latter authors did not relate the PSD to the calorimetric data.

Despite the relative clarity of the results presented in this study, the interpretation of the data is not easy. Four reasons can be mentioned. First, it was assumed that the degree of reaction, α, was proportional to the amount of heat released during the hydraulic reaction. This assumption is only valid when the exothermic α-TCP dissolution ($Ca_3(PO_4)_2 = 3Ca^{2+} + 2PO_4^{3-}$; −22.1 kJ/mol [10]) and the endothermic CDHA precipitation ($9Ca^{2+} + 6PO_4^{3-} + H_2O = Ca_9(HPO_4)(PO_4)_5OH$; 30.1 kJ/mol [10,11]) occur simultaneously. If there is a mismatch, the reaction rate is overestimated. To test the validity of the assumption, the crystallographic composition of cement pastes was

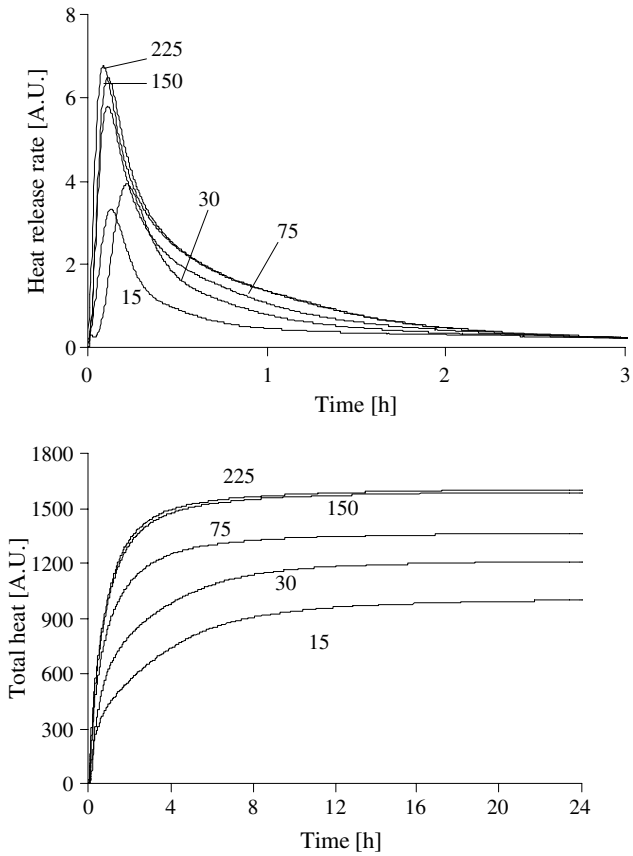

Fig. 4. Isothermal calorimetry curves of the second batch (see Table 1). Milling times: 15, 30, 75, 150 and 225 min. Top: frequency plot. Bottom: cumulative plot. The heat release rate and total heat are given in arbitrary units (raw signal in mV and mV s, respectively).

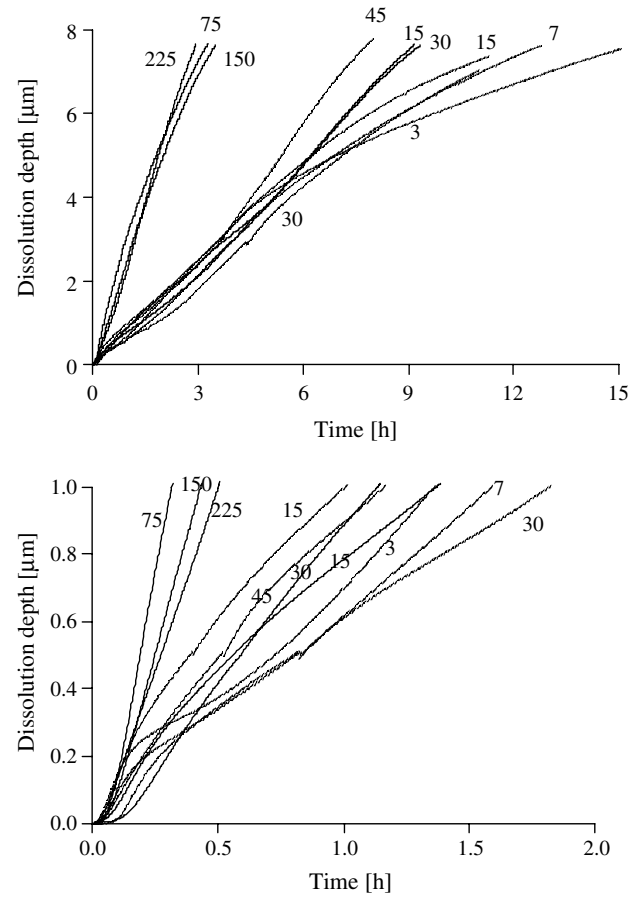

Fig. 5. Calculated dissolution depth as a function of time. The bottom chart is an enlargement of the top chart.

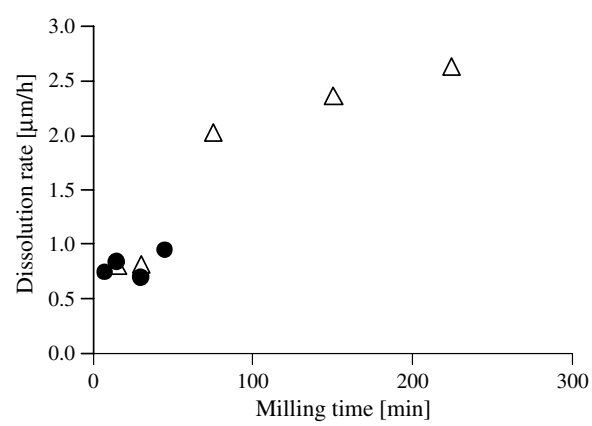

Fig. 6. Dissolution rate as a function of milling time: (●) batch 1; (△) batch 2.

determined applying the Rietveld refinement approach to X-ray diffraction spectra (the setting reaction was stopped at various times by grinding the paste in acetone). The dissolution rate obtained for powders 1024 (3 min milling time), 19 (15 min) and 1034 (150 min; Table 1) corresponded to 30%, 45% and 108% of the value obtained by calorimetry, respectively. Despite this large scattering in the data, it is likely that the assumption is correct because α-TCP solubility is very low (0.1 mM in pure water).

The second reason for the difficulty in analysing the data is the fact that the α-TCP powders tested in this study were in fact biphasic: they contained an X-ray well-crystallized phase and an X-ray amorphous phase [9]. The amorphous phase is likely to be more reactive and dissolve faster than the well-crystallized phase. For example, Gbureck et al. [8] observed that long-milled α-TCP powders were three times more soluble (apparent solubility) than standard α-TCP which could explain why the dissolution rate was increased threefold between short and long milling times (Fig. 6). To analyse the data, it would be necessary to know the composition of the α-TCP powder at each time point, which was not the case here.

The third reason for the difficulty in interpreting the data is the presence of a local minimum of particle size at an intermediate milling time suggesting particle agglomeration at long milling times (Table 1). This assumption is supported by the fact that despite an increase of particle size at long milling times, no change of specific surface area was measured. Moreover, the measured SSA values were much larger than the calculated SSA values (sometimes a sixfold difference), even though the particles appeared rather spherical (as seen by SEM; data not shown here).

These observations raise some concerns about the validity of the use of the PSD data for the calculation of the setting kinetics. The sharp increase of dissolution rate beyond 45 min milling time (Fig. 6) could be due to the separation of agglomerate into single particles during reaction.

The fourth and last aspect that complicates the interpretation of the data is the fact that most of the reaction occurred at a small dissolution depth. More precisely, 24–69% of the reaction was completed when the dissolution depth was 1 μm (Table 1; based on PSD data). A closer look at the data shows that in the range of dissolution depths between 0 and 1 μm, changes of slopes were observed (Fig. 5(bottom)). The initial "bump" seen along some of the curves is likely to be due to the wetting heat peak (assumed to be zero in the calculations).

Despite the uncertainties in the interpretation of the data, the approximately-linear behavior of all curves suggests that α-TCP conversion to CDHA is mostly a surface-controlled reaction, with at later stages a diffusion-controlled mechanism.

The dissolution rates measured in the present study are larger than previously-reported values: 0.08 [3], 0.09 and 0.14 μm/h [6] compared to at least 0.7–0.8 μm/h. The reason for this difference is unclear but is not surprising to those producing α-TCP powders regularly: batch to batch variability is often observed.

5. Conclusion

The kinetics of α-TCP hydraulic conversion to CDHA were determined for α-TCP powders milled for various durations. Reaction kinetics were calculated by combining particle size distribution data and isothermal calorimetry data. Results suggested that α-TCP conversion was initially controlled by surface reactions and in the later stages by diffusion (particularly for shortly milled powders). The presence of an X-ray amorphous α-TCP fraction in the crystalline α-TCP powder increased the dissolution rate threefold (from about 0.8 μm/h to about 2.5 μm/h), without modifying the reaction mechanism.

References

[1] Fernández E, Ginebra MP, Boltong MG, Driessens FCM, Ginebra J, DeMaeyer EAP, et al. Kinetic study of the setting reaction of a calcium phosphate bone cement. J Biomed Mater Res 1996;32:367–74.

[2] Ginebra MP, Fernández E, De Maeyer EA, Verbeeck RM, Boltong MG, Ginebra J, et al. Setting reaction and hardening of an apatitic calcium phosphate cement. J Dent Res 1997;76(4):905–12.

[3] Ginebra MP, Fernández E, Driessens FCM, Planell JA. Modeling of the hydrolysis of α-TCP. J Am Ceram Soc 1999;82(10):2008–12.

[4] Sarda S, Fernández E, Nilsson M, Balcells M, Planell JA. Kinetic study of citric acid influence on calcium phosphate bone cements as water-reducing agent. J Biomed Mater Res 2002;61(4):653–9.

[5] Durucan C, Brown PW. α-Tricalcium phosphate hydrolysis to hydroxyapatite at and near physiological temperature. J Mater Sci Mat Med 2000;11:365–71.

[6] Ginebra MP, Driessens FCM, Planell JA. Effect of the particle size on the micro and nanostructural features of a calcium phosphate cement: a kinectic analysis. Biomaterials 2004;25(17):3453–62.

[7] Durucan C, Brown PW. Reactivity of α-tricalcium phosphate. J Mater Sci 1999;37(5):963–9.

[8] Gbureck U, Barralet JE, Radu L, Klinger HG, Thull R. Amorphous alpha-tricalcium phosphate: preparation and aqueous setting reaction. J Am Ceram Soc 2004;87(6):1126–32.

[9] Camiré CL, Gbureck U, Hirsiger W, Bohner M. Correlating crystallinity and reactivity in an alpha-tricalcium phosphate. Biomaterials 2005;26(16):2787–94.

[10] Wyatt PAH. A thermodynamic bypass goto log *k*. Royal Society of Chemistry Monograph for Teachers, vol. 35. Cambridge: Royal Society of Chemistry; 1982.

[11] Martin RI, TenHuisen KS, Leamy P, Brown PW. Enthalpies of formation of compounds in the P_2O_5–CaO–H_2O system. J Phys Chem B 1997;101:9375–9.